Thermomechanical model and temperature measurements for shocked ammonium perchlorate single crystals

J. M. Winey, Y. A. Gruzdkov, Z. A. Dreger, B. J. Jensen, and Y. M. Gupta[a)]
Institute for Shock Physics and Department of Physics, Washington State University, Pullman, Washington 99164-2816

(Received 3 October 2001; accepted for publication 5 February 2002)

A consistent thermomechanical material model was developed for unreacted ammonium perchlorate (AP) single crystals for shock compression normal to the (210) and (001) crystal planes. Building on previous work, the mechanical response for both orientations was described using a single isotropic elastic-plastic model and an overstress model to describe rate-dependent yielding. Velocity interferometer measurements to 12 GPa were performed to extend the AP Hugoniot curve to higher stresses. The specific heat c_v, the coefficient of thermal pressure $(\partial P/\partial T)_V$, and the isothermal bulk modulus B_T were determined from Hugoniot and isothermal compression curves, along with available data at atmospheric pressure. Time-resolved Raman spectroscopy experiments were carried out under stepwise loading to obtain temperatures in the shocked state. Calculated temperatures using our material model are in good agreement with the temperatures obtained from our experiments, thus providing validation for our modeling approach. © *2002 American Institute of Physics.* [DOI: 10.1063/1.1465118]

I. INTRODUCTION

Interpreting and modeling data from experiments designed to examine shock-induced chemical decomposition of energetic materials requires knowledge of the thermodynamic and mechanical response of the material. In particular, the ability to calculate temperature in the shocked material is important for analyzing chemical mechanisms and kinetics. For this reason, good thermomechanical models of unreacted energetic materials represent an important need.

Because of the importance of ammonium perchlorate (AP) as an oxidizer in propellants, its decomposition has been studied under atmospheric pressure[1,2] and static high pressure[3] conditions, as well as under shock wave loading.[4,5] In recent work in our laboratory, the mechanical response of AP single crystals to plane shock wave loading was examined using quartz gauges to measure wave profiles to stresses of 6 GPa.[6] Using the wave profile data, a rate-dependent, elastic-plastic material model was constructed to describe the shock response of AP. However, despite these efforts,[1–6] little work has been done to characterize the thermodynamic response of shocked AP crystals. In a recent study of liquid nitromethane,[7] a method was developed for constructing a complete equation of state (EOS) from available experimental data. Here, this method is extended to crystals such as AP.

In the present work, our objective was to develop a consistent material description for unreacted AP single crystals, describing both the mechanical and thermodynamic properties of the shocked material. To achieve this goal, we extended the previous mechanical models[6] for AP to higher stresses. We also incorporated a thermodynamic description using a method similar to the previous development for nitromethane.[7] Because temperature calculations are quite sensitive to the EOS models used,[7] we performed Raman scattering experiments to obtain temperatures in shocked AP crystals. These measurements provide a stringent test of our material description.

In this article, we give a complete description of work that was partially presented in an earlier report.[8] In the following section, we present the development of our material model. Section III contains the experimental methods and analysis for obtaining temperature using Raman scattering experiments. In Sec. IV, we discuss predictions of our material model and the results of our temperature measurements. A summary is given in Sec. V.

II. THERMOMECHANICAL MODEL DEVELOPMENT

A. Overall approach

A proper description of the mechanical and thermodynamic properties of single-crystal AP requires a tensor formulation that reflects the symmetry of the crystal (orthorhombic, Pnma space group).[9] However, following previous work,[6] we assumed that each orientation of the AP crystal can be described by a single isotropic material model, since the two orientations considered [(210) and (001)] have similar shock responses. The stresses were conveniently expressed as the sum of the compressive mean stress $\bar{P}$ and the stress deviators s_{ij},

$$\sigma_{ij} = -\bar{P}\delta_{ij} + s_{ij}, \tag{1}$$

where the stresses are positive in tension. Material strength was assumed to be independent of the mean stress and plastic deformation was taken to be incompressible. We also assumed that the mean stress is equivalent to the thermodynamic pressure, and the elastic response is described by bulk and shear moduli.

a)Electronic mail: ymgupta@wsu.edu

As before,[6] the rate dependence of AP was described using a simple overstress model, where the plastic strain rate is given in terms of the second invariant of the deviatoric stress tensor $\sqrt{J_2'}$:

$$\dot{\epsilon}_{ij}^{P}=\frac{s_{ij}^{(i)}}{2GT_R}\left[1-\frac{\sqrt{J_2'^{(e)}}}{\sqrt{J_2'^{(i)}}}\right]. \tag{2}$$

Here (i) denotes the instantaneous stress, (e) denotes the equilibrium value at the yield surface, G is the shear modulus, and T_R is the characteristic relaxation time. Because the work done by plastic deformation is primarily unrecoverable, we assumed it to be completely dissipated as heat. This irreversible heat production was included as a contribution to the total entropy production under shock wave loading.

Similar to the previous work on liquid nitromethane,[7] the thermodynamic response was described by modeling the specific heat c_v, the coefficient of thermal pressure $(\partial P/\partial T)_V$, and the isothermal bulk modulus B_T as functions of temperature and volume. The specific heat was described in terms of Einstein oscillators since the internal vibrational modes of the ammonium and perchlorate ions are of primary concern for temperatures greater than 298 K. $(\partial P/\partial T)_V$ was determined from the difference between the Hugoniot and isothermal compression curves in the $P-V$ plane, whereas the isothermal compression curve and thermodynamic consistency relationships were sufficient to determine B_T.

B. Mechanical response

To extend the Hugoniot curve for AP, previous quartz gauge data[6] at stresses up to 6 GPa were augmented with the results of four velocity interferometer measurements that we performed to stresses as high as 12 GPa. The experimental details regarding these measurements are similar to those of Ref. 10. Briefly, a copper impactor mounted on a projectile was accelerated using either a light gas gun or a powder gun. The copper plate impacted a target assembly consisting of an AP single crystal contained between two [100]-oriented LiF windows, as shown schematically in Fig. 1(a). The interface between the AP sample and the LiF back window had a vapor-coated aluminum film to provide a mirror for interferometry. The velocity of this mirror surface was measured during the experiment using our velocity interferometer system.[10] The results of our experiments are shown in Table I.

Since our interferometry data provide particle velocities at the mirror interface, Hugoniot points in the $P-V$ plane were determined using wave propagation calculations as follows. The particle velocity data and the quartz gauge data[6] were simulated using a wave propagation code,[11] a cubic polynomial relationship between pressure (mean stress) and the compression parameter, $\mu=V_0/V-1$, and the appropriate strength model. The simulations were repeated with adjusted polynomial coefficients until the $P-\mu$ relationship converged to a best fit of the combined quartz gauge and particle velocity data. The mean stress curve corresponding to the Hugoniot using this procedure is

$$P_H=16.08\mu+41.70\mu^2+63.28\mu^3 \ \ (\text{GPa}). \tag{3}$$

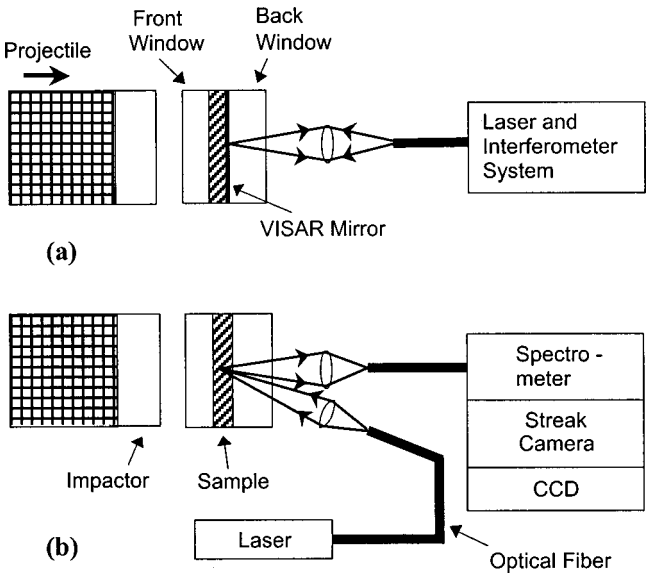

FIG. 1. Diagram of experimental configuration for: (a) velocity interferometer experiments, (b) Raman scattering experiments.

The first coefficient in Eq. (3), the isentropic bulk modulus at ambient pressure, was held constant in the fitting process. Its value was inferred by averaging[12] the measured elastic constants of AP.[13] We retained the same value for the shear modulus ($G=14.19$ GPa) as in the previous work.[6] In addition, our values for the yield parameters in Eq. (2) ($\sqrt{J_2'^{(e)}}=0.2078$ GPa and $T_R=5$ ns) are similar to those in Ref. 6.

Simulations of the quartz gauge wave profiles using our mechanical model gave results similar to those of Ref. 6. However, in contrast to the previous model,[6] the present model provided good fits to the particle velocity profiles to 12 GPa. In Fig. 2, the mean stress curve from Eq. (3) is compared with the one given in Ref. 6. In the pressure range of the quartz gauge data (up to 6 GPa), the two curves are indistinguishable. However, the two curves diverge at higher pressures, since our particle velocity measurements showed that the Hugoniot response of AP above 6 GPa is less stiff than previously thought.

C. Thermodynamic response

We assume the specific heat c_v for AP to be independent of volume, describing it as the sum of three Einstein oscillators:

$$c_v(T)=A_1E(\theta_1/T)+A_2E(\theta_2/T)+A_3E(\theta_3/T), \tag{4}$$

where

$$E(x)=\frac{x^2e^x}{(e^x-1)^2}.$$

The three oscillators are used to independently account for low, intermediate, and high frequency vibrational modes of the crystal. The parameters A_3 and θ_3 were determined by assigning the high frequency oscillator to the high frequency stretching modes of the NH_4^+ ion ($\nu>3200$ cm^{-1}).[14] The remaining parameters were determined by fitting Eq. (4) to available specific heat data,[15] in which $c_p(T)$ was converted

TABLE I. Particle velocity measurements for shocked AP.

Expt. no. crystal orientation[a]	Sample thickness (mm)	Impact velocity (km/s)	Experimental configuration: impactor —buffer—sample —back window	Measured interface velocity after initial shock[b] (km/s)	AP Hugoniot particle velocity[c] (km/s)	AP Hugoniot pressure[c] (GPa)
V1 (210)	1.99	1.150	Cu–LiF–AP–LiF	0.777	1.025	9.16
V2 (210)	0.47	1.444	Cu–LiF–AP–LiF	0.986	1.263	12.24
V3 (001)	1.97	1.174	Cu–LiF–AP–LiF	0.794	1.045	9.40
V4 (001)	0.48	1.419	Cu–LiF–AP–LiF	0.961	1.243	11.99

[a]The crystal orientation is described by the Miller indices of the plane of impact.
[b]In all these experiments, the elastic precursor was overdriven. The measured particle velocity is less than the Hugoniot particle velocity because the measurement was taken at the AP/LiF interface [see Fig. 1(a)].
[c]Hugoniot particle velocities and pressures were determined using wave code calculations (Ref. 11), as described in Sec. II. Along the Hugoniot curve, the longitudinal stress (positive in compression) and pressure are related by $P_x = P + 2\sqrt{J_2'}/\sqrt{3}$.

to $c_v(T)$ using other thermodynamic data.[13,16] The Dulong–Petit value for AP ($c_v = 2.123\,\mathrm{J/g\,K}$) was used to constrain the fit of Eq. (4) in the high temperature limit. The result of the fit is shown in Fig. 3.

Because our c_v model is independent of volume, the coefficient of thermal pressure $(\partial P/\partial T)_V$ must be independent of temperature through the consistency relationship

$$\frac{1}{T}\frac{\partial c_v}{\partial V} = \frac{\partial}{\partial T}\left(\frac{\partial P}{\partial T}\right)_V. \tag{5}$$

Therefore, along a constant volume path,

$$\left(\frac{\partial P}{\partial T}\right)_V = \left.\frac{P_2 - P_1}{T_2 - T_1}\right|_V. \tag{6}$$

Hence, if pressure and temperature are known along two curves in the $P-V$ plane, $(\partial P/\partial T)_V$ can be determined at any volume by evaluating Eq. (6) along a constant volume path from one curve to the other, as illustrated in Fig. 4.

As before,[7] it is convenient to use the mean stress corresponding to the Hugoniot and the isothermal compression response to determine $(\partial P/\partial T)_V$ for AP. The mean stress along the Hugoniot curve was taken from Eq. (3), while the isothermal compression curve was obtained from a third-order Birch–Murnaghan (B–M) fit[17] to the data of Peiris *et al.*[18] For the B–M fit, the isothermal bulk modulus was held constant at $B_0 = 15.16\,\mathrm{GPa}$. This value was inferred from the measured isentropic elastic constants,[13] after thermodynamic correction for isothermal conditions.[19] The best fit value for the second B–M parameter is $B' = 6.4$. Although we used the isothermal data of Peiris *et al.*, the B–M parameters obtained from our fit to their data differ significantly from their parameters.[20]

To evaluate Eq. (6), the Hugoniot temperature T_H is required. Since the Hugoniot temperature depends on $(\partial P/\partial T)_V$, T_H and $(\partial P/\partial T)_V$ were determined simultaneously by iteration. The resulting values of $(\partial P/\partial T)_V$ as a function of volume are shown in Fig. 5. To provide an analytical representation for $(\partial P/\partial T)_V$, the curve in Fig. 5 was fitted with a polynomial. Because $(\partial P/\partial T)_V$ was determined from the Hugoniot and isothermal compression curves, our model is applicable to the region of the $P-V$ plane bounded by these two curves.

Using our models for c_v and $(\partial P/\partial T)_V$, the Gruneisen coefficient Γ/V was calculated using the thermodynamic relationship

$$c_v\frac{\Gamma}{V} = \left(\frac{\partial P}{\partial T}\right)_V. \tag{7}$$

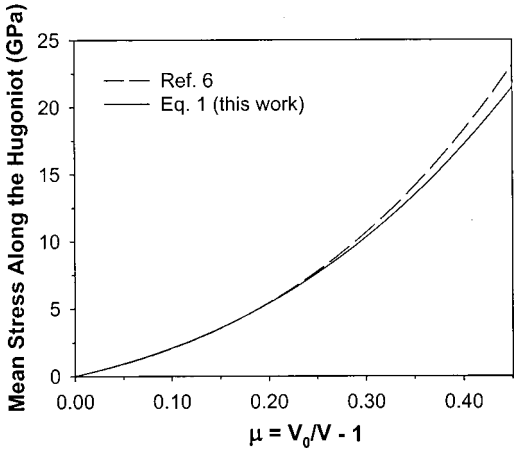

FIG. 2. Mean stress–compression curves along the Hugoniot for AP.

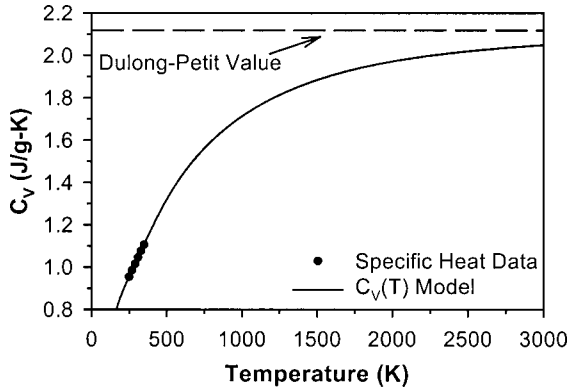

FIG. 3. Specific heat c_v vs temperature. The model approaches the Dulong–Petit value in the high temperature limit.

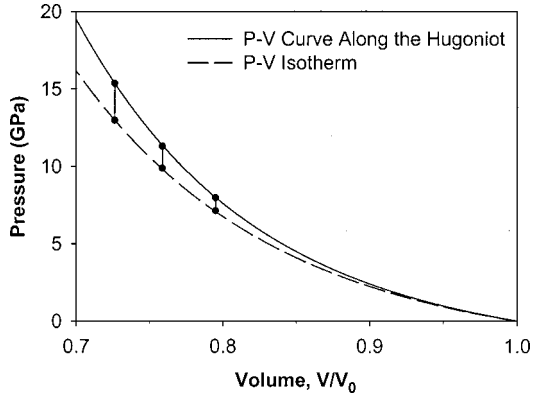

FIG. 4. Mean stress–compression curve along the Hugoniot and isothermal compression curve for AP. The vertical lines represent paths of constant volume between the two curves.

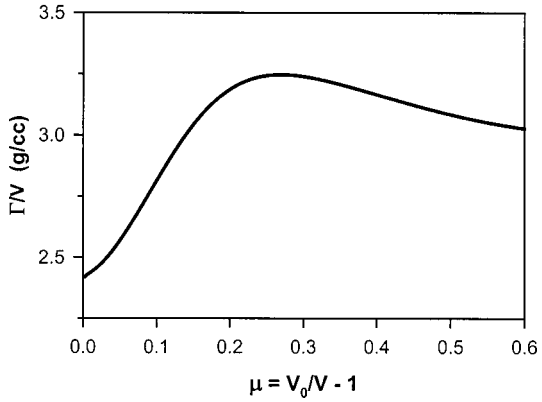

FIG. 6. Gruneisen coefficient Γ/V versus compression along the Hugoniot curve.

Since our model for c_v is independent of volume, the behavior of Γ/V under isothermal compression is proportional to that of $(\partial P/\partial T)_V$ in Fig. 5. However, because both c_v and $(\partial P/\partial T)_V$ increase under shock compression, the behavior of Γ/V along the Hugoniot curve is as shown in Fig. 6. The nonmonotonic behavior of Γ/V in the figure is a result of competition between the temperature dependence of c_v and the volume dependence of $(\partial P/\partial T)_V$. Further discussion regarding the behavior of Γ/V can be found in our nitromethane paper.[7] Because the B–M isotherm used to determine $(\partial P/\partial T)_V$ represents an extrapolation beyond the isothermal data, caution is needed in interpreting the shape of the curves in Figs. 5 and 6.

The isothermal bulk modulus B_T was determined by integrating the consistency relationship

$$\frac{\partial B_T}{\partial T} = -V\frac{\partial}{\partial V}\left(\frac{\partial P}{\partial T}\right)_V \tag{8}$$

with respect to temperature. Since our model for $(\partial P/\partial T)_V$ is independent of temperature,

$$B_T(T,V) = B_T(T_0,V) - V(T-T_0)\frac{\partial}{\partial V}\left(\frac{\partial P}{\partial T}\right)_V. \tag{9}$$

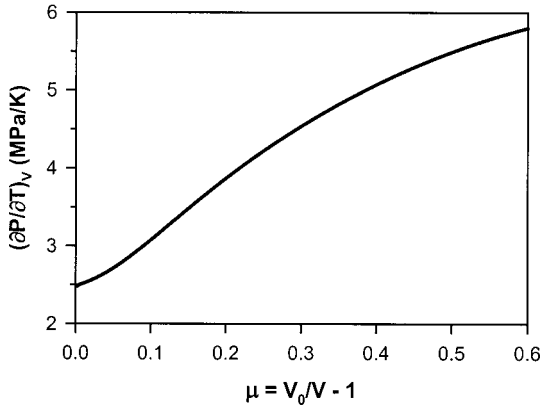

FIG. 5. Coefficient of thermal pressure $(\partial P/\partial T)_V$ versus compression.

In this expression, the first term is obtained from the B–M isothermal compression curve and the second term is derived from the polynomial fit to the $(\partial P/\partial T)_V$ values.

III. TEMPERATURE MEASUREMENTS

To test and constrain our EOS models, we performed time-resolved Raman spectroscopy experiments on AP crystals to measure temperature under step-wise loading conditions. Using the method developed previously,[21] the intensity of the Stokes and anti-Stokes peaks for a given vibrational mode were measured simultaneously. The temperature was derived from the ratio of the anti-Stokes and Stokes intensities,[22]

$$\frac{I_{as,\omega_V}}{I_{s,\omega_V}} = \frac{(\omega_L+\omega_V)^4}{(\omega_L-\omega_V)^4}\exp\left(\frac{-\hbar\omega_V}{k_BT}\right), \tag{10}$$

where I_{as,ω_V} and I_{s,ω_V} are the anti-Stokes and Stokes intensities, respectively, collected over the same scattering solid angle and volume for a particular vibrational mode of the material with energy $\hbar\omega_V$, ω_L is the laser excitation frequency, k_B is the Boltzmann constant, and T is temperature.

Details of the experimental method are given in Ref. 21. Briefly, the AP sample (400–500 μm thick) was bounded by two optical windows ([100]-oriented LiF or a-cut sapphire), as shown in Fig. 1(b). Since epoxy bonds are susceptible to damage by the excitation laser, liquid nonane was used to fill the gaps between the sample and the windows. Nonane was chosen for its chemical stability and its low vapor pressure. The thickness of the nonane layer was typically $\sim$5 μm. The sample cell was impacted by a flyer plate accelerated using a single-stage gas gun. Upon impact, the resulting shock wave traveled through the front window and into the sample. As the shock wave reverberated in the sample between the two windows, the sample was subjected to step-wise loading under uniaxial strain.

During the experiment, laser light (flashlamp-pumped pulsed dye laser, $\lambda_L = 514$ nm) scattered from the sample was collected using optical fibers and passed through a holographic notch filter to attenuate the elastically scattered light. The remaining signal was delivered to a spectrometer/streak

TABLE II. Temperature measurements and calculated temperatures for shocked AP.[a]

Expt. no./ crystal orientation[b]	Impact velocity (km/s)	Experimental configuration: impactor—buffer and/or front window—sample—back window	Calculated final pressure (GPa)	Calculated final temperature (K)	Experimental temperatures (K)		
					627 cm^{-1} mode	933 cm^{-1} mode	Average temp.
T1 (210)	1.138	Cu–Cu/LiF–AP–LiF	13.0	593	638± 89	584±81	611±60
T2 (210)	1.132	Sapphire–LiF–AP–LiF	13.5	604	646±104	583±55	615±59
T3 (210)	1.180	Sapphire–LiF–AP–LiF	14.2	624	656±109	632±93	644±72
T4 (210)	0.886	Sapphire–LiF–AP–Sapphire	16.1	593	535±124	636±37	588±65
T5 (001)	1.124	Sapphire–LiF–AP–LiF	13.5	605	615±119	605±89	610±74
T6 (001)	0.906	Sapphire–LiF–AP–Sapphire	16.5	602	590±106	608±54	599±59

[a]The thickness of all AP samples ranged from 400–500 μm.
[b]The crystal orientation is described by the Miller indices of the plane of impact.

camera/charge coupled device detection system. The resulting Raman spectra were acquired with 50 ns time resolution until the experiment was terminated by the arrival of edge release waves at ~800 ns after impact.

Selected spectra from Experiment T6 (see Table II) are shown in Fig. 7. The spectra consist of Stokes and anti-Stokes peaks from three vibrational modes. The peaks at negative wave numbers are the anti-Stokes peaks. The three modes shown are the symmetric ClO_4^- stretch (A_1) at 933 cm^{-1}, and ClO_4^- bending modes at 627 cm^{-1} (T_2) and 461 cm^{-1} (E), using the assignments from Ref. 14. Spectrum A of Fig. 7 was collected under ambient pressure conditions. Spectrum B was collected from the shocked sample after the final pressure state was reached. Under shock conditions, the Raman peaks broaden and shift to higher vibrational frequency. However, the anti-Stokes peaks also gain intensity relative to the Stokes peaks, reflecting the temperature increase due to shock compression.

To obtain temperatures from the Raman data, the time-resolved spectra corresponding to the final compression state of the AP were averaged. The averaged spectrum was analyzed by fitting the peaks with Gaussian functions, as described in Ref. 21. Raman scattering intensities were assumed proportional to the area under the peaks. The anti-Stokes/Stokes intensity ratios were then used to infer temperatures according to Eq. (10). Due to difficulties in background subtraction, the 461 cm^{-1} peak was not used to infer temperature. The uncertainty in the temperature values was estimated by obtaining temperatures from each time-resolved spectrum separately. The standard deviation of this set of temperature values is the reported uncertainty.

The results of six different step-wise loading experiments are shown in Fig. 8 and Table II. We believe that the ~10% uncertainties shown represent overestimates but an objective method for obtaining more realistic uncertainty estimates has not been developed to date. The temperatures shown do not increase monotonically with final pressure because the use of different experimental configurations results in different thermodynamic compression states for a given final pressure.[23] The four experiments at lower pressures utilized LiF windows on both sides of the sample. The two experiments at higher pressure had a sapphire back window.

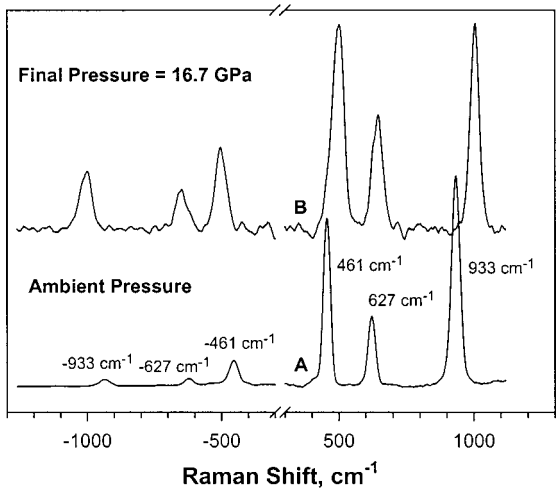

FIG. 7. Background-subtracted Raman spectra of AP from Exp. T6. These spectra were obtained by averaging individual time-resolved spectra collected at ambient pressure (Spectrum A) or at a final pressure of 16.7 GPa (Spectrum B).

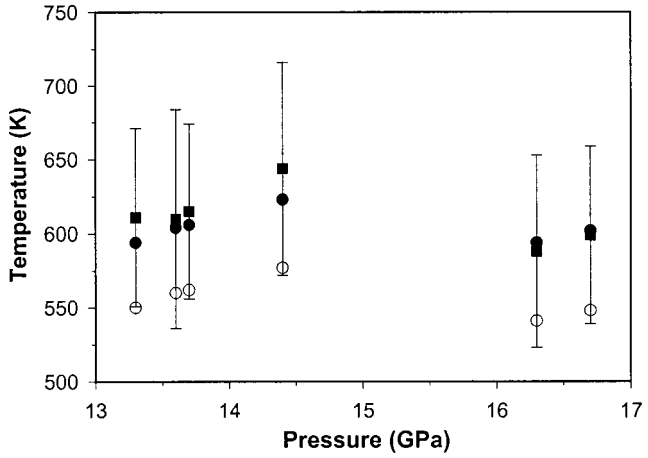

FIG. 8. Temperatures at peak pressures under stepwise loading conditions. The filled squares represent temperatures inferred from our Raman scattering experiments. The error bars shown are likely overestimates of the experimental uncertainty. Also shown are temperature predictions from EOS models developed using the isothermal compression data of Ref. 18 (filled circles) or Ref. 24 (open circles).

IV. DISCUSSION

Calculated temperatures, using our EOS models, are shown in Fig. 8 (filled circles) and Table II, and are compared with our experimentally obtained values (filled squares). Our EOS predictions show good agreement with the temperatures inferred from the Raman spectroscopy experiments, thus providing an important validation of our EOS model. The small degree of scatter between the measured and calculated temperatures supports our suggestion that the error bars indicated for the measured temperatures are overestimates.

In our earlier report,[8] the isothermal compression data of Sandstrom *et al.*[24] were used to construct the EOS models. The calculated temperatures from these earlier developments, shown in Fig. 8 as the open circles, are significantly lower than the experimentally obtained temperatures. This difference is caused by the inability to obtain a good constraint to the B–M isotherm from the work of Sandstrom *et al.*[24] because their data were quite limited and displayed considerable scatter. Therefore, we had previously adjusted the B–M isotherm to fit our temperature data and the resulting parameters for the B–M fit were[8]

$$B_0 = 15.16 \text{ GPa}, \quad B' = 6.4. \tag{11}$$

These parameters are the same as those obtained by us from the isothermal compression data of Peiris *et al.*,[18] as indicated in Sec. II of this article. This agreement demonstrates that, in the absence of accurate isothermal $P-V$ data, temperature measurements can be used effectively to constrain EOS developments.

It is noteworthy that a single isotropic material model is able to describe the shock response for two different orientations of AP single crystals. This is likely due to two factors: the low yield stress of AP keeps the stress deviators small and the mean stress under shock compression is similar for the two orientations. For highly anisotropic energetic crystals such as PETN, these conditions are not met and an isotropic model is expected to be inadequate for describing the shock response along different crystal orientations.

In previous static high pressure work,[18] evidence was presented for a structural phase transition at 3 GPa to a crystalline phase of unknown symmetry. However, shock wave profiles both in the previous quartz gauge measurements[6] and current particle velocity measurements show no features characteristic of a phase transition. This suggests that the phase transition occurs either with a negligible change in volume or with very slow kinetics. The good agreement of our temperature calculations with our experimentally obtained temperatures provides independent support for this suggestion since the mean stress curve corresponding to the Hugoniot and the isothermal compression curve used in our EOS development assume no discontinuous volume changes in the $P-V$ plane.

V. CONCLUSIONS

A consistent thermomechanical material description for shocked AP single crystals was developed using thermodynamic and mechanical data to constrain the models. Simulations using this material model agree well with wave profile data to 12 GPa. Temperature predictions using our model are in agreement with temperatures inferred from the Raman spectroscopy measurements to pressures approaching 17 GPa. With our EOS development approach, temperature calculations depend strongly on the $P-V$ compression data used to construct EOS models. Accurate $P-V$ compression data are therefore needed. When the isothermal $P-V$ data are questionable, temperature measurements under stepwise shock wave loading provide an important constraint on the EOS models.

The material model developments presented here are expected to be applicable to other energetic crystalline materials that do not display a strongly anisotropic response under shock wave loading.

ACKNOWLEDGMENTS

D. Savage and K. Zimmerman are thanked for their very capable assistance with the experiments. T. L. Boggs is gratefully acknowledged for providing the AP crystals used in our experiments. This work was supported by the Office of Naval Research and the Lawrence Livermore National Laboratory.

[1] P. W. M. Jacobs and H. M. Whitehead, Chem. Rev. **69**, 551 (1969).
[2] P. W. M. Jacobs and G. S. Pearson, Combust. Flame **13**, 419 (1969).
[3] G. I. Pangilinan and T. P. Russell, in *Shock Compression of Condensed Matter—1997*, edited by S. C. Schmidt, D. P. Dandekar, and J. W. Forbes (AIP Press, New York, 1998), p. 809.
[4] W. L. Elban, H. W. Sandusky, B. C. Beard, and B. C. Glancy, J. Propul. Power **11**, 24 (1995).
[5] H. W. Sandusky, B. C. Glancy, D. W. Carlson, W. L. Elban, and R. W. Armstrong, J. Propul. Power **7**, 518 (1991).
[6] G. Yuan, R. Feng, Y. M. Gupta, and K. Zimmerman, J. Appl. Phys. **88**, 2371 (2000).
[7] J. M. Winey, G. E. Duvall, M. D. Knudson, and Y. M. Gupta, J. Chem. Phys. **113**, 7492 (2000).
[8] J. M. Winey, Z. A. Dreger, Y. A. Gruzdkov, B. J. Jensen, and Y. M. Gupta, in *Shock Compression of Condensed Matter—1999*, edited by M. D. Furnish, L. C. Chhabildas, and R. S. Hixson (AIP Press, New York, 2000), p. 231.
[9] C. S. Choi, H. J. Prask, and E. J. Prince, J. Chem. Phys. **61**, 3523 (1974).
[10] S. C. Jones and Y. M. Gupta, J. Appl. Phys. **88**, 5671 (2000).
[11] COPS, 1-D finite difference wave code, Y. M. Gupta (Stanford Research Institute, Menlo Park, 1978) (unpublished).
[12] See, for example, J. P. Hirth and J. Lothe, *Theory of Dislocations* (McGraw–Hill, New York, 1968), p. 399. The elastic constants were averaged according to both the Voigt and Reuss methods. Since these two methods provide upper and lower bounds, respectively, for the bulk modulus, the Voigt and Reuss values were averaged to yield the value in Eq. (3).
[13] S. Haussuhl, Z. Kristallogr. **192**, 137 (1990).
[14] T. B. Brill and F. Goetz, J. Chem. Phys. **65**, 1217 (1976); T. B. Brill and F. Goetz, in *Experimental Diagnostics in Combustion of Solids*, edited by T. L. Boggs and B. T. Zinn (American Institute of Aeronautics and Astronuatics, New York, 1978), p. 3.
[15] E. F. Westrum and B. H. Justice, J. Chem. Phys. **50**, 5083 (1969).
[16] H. J. Prask, C. S. Choi, N. J. Chesser, and G. J. Rosasco, J. Chem. Phys. **88**, 5106 (1988).
[17] F. Birch, J. Geophys. Res. **83**, 1257 (1978).
[18] S. M. Peiris, G. I. Pangilinan, and T. P. Russell, J. Phys. Chem. A **104**, 11188 (2000).
[19] D. C. Wallace, *Thermodynamics of Crystals* (Wiley, New York, 1972).
[20] In our fit, we used isothermal data to 3 GPa despite some suggestions of a phase transition at 0.9 GPa (Ref. 18). This is justified by the apparent lack of either a discontinuous volume change or a change in crystal structure at 0.9 GPa in the x-ray diffraction data of Ref. 18.

[21] G. I. Pangilinan and Y. M. Gupta, J. Appl. Phys. **81**, 6662 (1997).
[22] H. Poulet and J. P. Mathieu, *Vibration Spectra and Symmetry of Crystals* (Gordon and Breach, New York, 1976).
[23] J. M. Winey and Y. M. Gupta, J. Phys. Chem. A **101**, 9333 (1997).
[24] F. W. Sandstrom, P. A. Persson, and B. Olinger, in *Tenth International Detonation Symposium* (Office of Naval Research, Arlington, VA, 1995), p. 766.